Porous LSCO Electrode Fabricated with Pulsed Laser Deposition for Advanced Thin Film Fuel Cell Application

X. CHEN, J. R. LI, L. SMITH, Y. Q. WANG, N. J. WU, AND A. IGNATIEV
Center for Advanced Materials and Department of Physics
University of Houston
Houston, TX 77204
USA

Abstract: - $La_{0.5}Sr_{0.5}CoO_{3-\delta}$ (LSCO) electrodes of a porous/dense composite layered structure were fabricated on both sides of a YSZ (111) substrate by pulsed laser deposition. SEM and AFM analysis indicated the outer layer of the LSCO is of micro/nano porous structure and the inner layer is dense. Impedance spectroscopy analysis was performed on the LSCO/YSZ/LSCO sample from 300 to 600°C in air. The electrode area specific resistance was found to be ~1Ω·cm^2 at 600°C and was extrapolated to <0.1Ω·cm^2 for temperatures of ~700°C, indicating a good potential for the LSCO thin films to be used in applications such as the intermediate temperature thin film solid oxide fuel cells.

Key-words: - Fuel Cell, Cathode, Pulsed Laser Deposition

1 Introduction

A goal in current solid oxide fuel cell (SOFC) research is to reduce fuel cell operation temperature to an intermediate temperature range of 700°C or lower. This is a challenge due to the relatively high activation energy for oxygen reduction, and hence requires particular attention in the choice of cathode material for the fuel cell [1]. $La_{0.5}Sr_{0.5}CoO_{3-\delta}$ (LSCO) is a mixed ionic-electronic conducting oxide (MIEC), which has found application as cathode material for solid oxide fuel cells; however lower temperature operation as that found in thin film fuel cells [2] may require increased porosity to improve LSCO cathode properties. In this paper, we report our study of porous/dense LSCO multilayer thin films for SOFC applications.

2 Experimental

LSCO thin films in a composite layered structure were deposited by pulsed laser deposition (PLD) symmetrically on both sides of a double-side polished 500μm thick YSZ (111) single crystalline wafer substrate. A KrF excimer laser was used for the deposition with pulse energy of 630mJ. The LSCO films were comprised of an inner layer of ~200nm thickness and an outer layer of ~6000nm thickness. Each of the inner layers was deposited at a temperature of ~500°C for 15min, and each of the outer layers was deposited at room temperature for 30min [3].

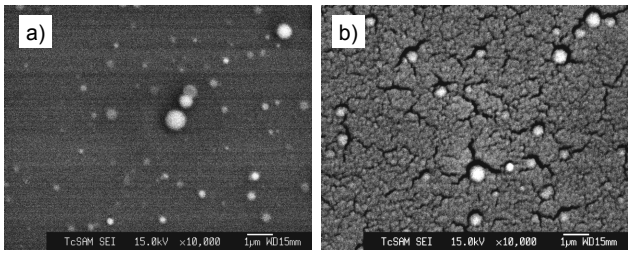

Fig.1 SEM of a) the dense bottom LSCO layer; and b) the top of the PLD made porous LSCO film.

An SEM micrograph of the surface of the inner layer before the outer layer was grown is shown in Fig.1(a), and indicates a dense pore-free LSCO layer with limited micro particles on the surface. An SEM micrograph of the outer layer after it was grown on top of the inner layer is shown in Fig.1(b), and indicates that the outer

layer is porous with micro/nano pores. These SEM results indicate that the LSCO structure is a composite film with an outer micro/nano porous layer on inner dense layer.

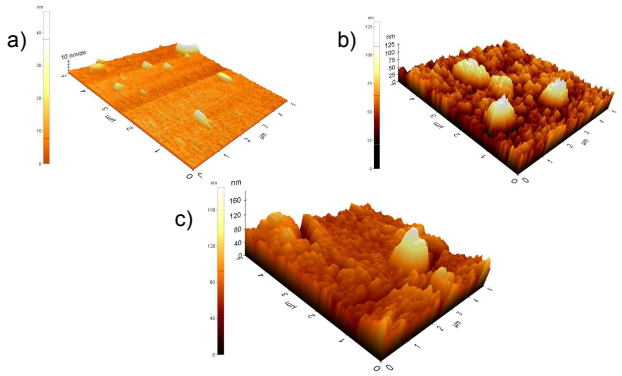

Fig.2 AFM measurements of a) the dense inner layer; b) the micro-nano porous outer layer; and c) the annealed surface of the porous film.

AFM measurements shown in Fig.2(a) indicate the topography of the dense inner layer to have general area smoothness close to atomic level. Fig.2(b) is the AFM scan of the micro-nano porous outer layer, with the surface seen to be covered by ~100nm size pores. Annealing the sample at 650°C resulted an agglomerative effect with deeper and longer pores in the layer as shown by SEM (Fig.2(c)). However, AFM measurements show that the local microscopic surface roughness of the LSCO film is similar before and after heating as demonstrated in Fig.3. The grains grow a little larger and pores become a little deeper. Therefore, the LSCO film surface remains nano porous.

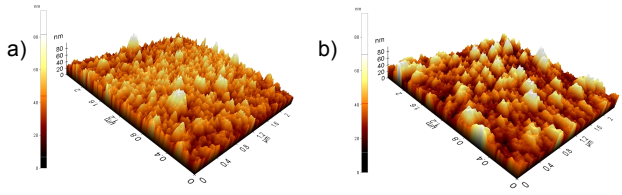

Fig.3 AFM measurement on the porous LSCO film in more detail a) before and b) after annealing.

XRD analysis of the LSCO composite film is shown in Fig.4. Fig.4(a) is the XRD of the LSCO composite film as grown. Judging by the very weak (200) peak, it can be concluded that the film is weakly (100) oriented. This is expected since for the purpose of increasing porosity of the LSCO film for electrode applications, the structure was intentionally not deposited at high epitaxial growth temperatures. Fig.4(b) is the XRD of the LSCO after annealing and in comparison with Fig.4(a), an extra LSCO(110) peak is seen, indicating a weak crystallization in the film as a result of heating. Yet, these LSCO peaks are still low and the film is best qualified to be principally polycrystalline.

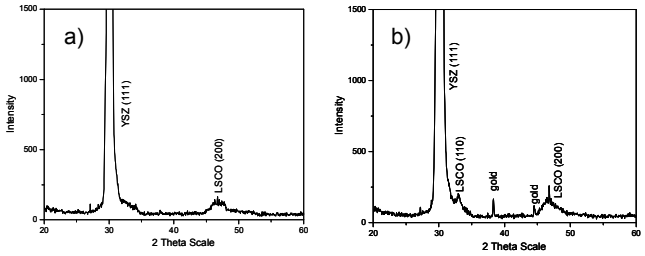

Fig.4 XRD of the composite LSCO film a) before and b) after annealing.

Impedance spectroscopy analysis was performed on the above LSCO/YSZ/LSCO sample in the temperature range from 400 to 650°C in air. Care was taken to stabilize the temperature before the impedance measurements were made. A representative impedance plot obtained on the sample and the analysis on it is shown in Fig.5. The distinctive features of the ionic conduction of the YSZ electrolyte and the oxygen exchange on the LSCO electrode surface were observed on the impedance spectra. As shown in Fig.5(a), the dotted curve is the measured data of the sample taken at 450°C. Its left semicircle corresponds to the YSZ bulk ion conductivity, and the right semicircle is due to the LSCO composite electrode. The interfacial impedance between the bulk and the electrode is small and hardly discerned in the diagram. Fig.5(b) is the equivalent circuit of the sample, where Rs is the resistance of the sample leads, R1 is the resistance of the YSZ bulk and CPE is a constant-phase element representing the

capacitive contribution of the YSZ bulk, GE represents the impedance of the LSCO electrodes. We point out that the dense LSCO layers should have little contribution to the impedance of the electrode. Its main function is to improve oxygen transportation into and out of the YSZ layer, so as to greatly reduce the interface impedance. Due to the low interface impedance and the low LSCO dense layer impedance, the total electrode impedance can be principally represented by the impedance of the LSCO porous electrode alone, which has the form [4]:

$$Z_{chem}=R_{chem}(1+jwt_{chem})^{-1/2} \quad (1)$$

where R_{chem} and t_{chem} can be defined by:

$$t_{chem}=1/GE_P \quad (2.1)$$

$$R_{chem}=1/(GE_T GE_P^{1/2}) \quad (2.2)$$

and GE_P and GE_T are the Gerischer fitting elements. Choosing appropriate values for GE_P and GE_T yield the fit shown as the solid line in Fig.5(a).

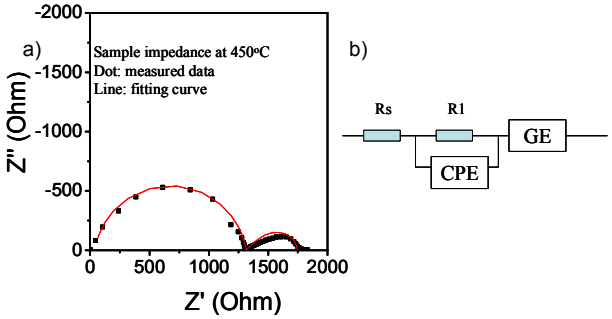

Fig.5 a) LSCO/YSZ/LSCO sample impedance analysis at 450°C and b) its equivalent circuit fitting model.

Fig.6 presents the temperature dependence for the resistivity values of the YSZ bulk and LSCO electrodes, respectively, using the impedance measurement data. As can be seen in the figure, the activation energy of LSCO electrode surface resistivity is higher than that of the YSZ bulk ion resistivity, with a value of ~136kJ/mol. The surface resistivity of the LSCO electrode is ~1Ω·cm at 600°C, and is extrapolated to be <~0.1Ω·cm for temperatures >700°C, which is much lower than what we obtained on a dense LSCO film (downward triangle point in the figure). This indicates a good potential for the LSCO thin film to be utilized in applications such as the intermediate temperature ultra thin solid oxide fuel cells [5,6].

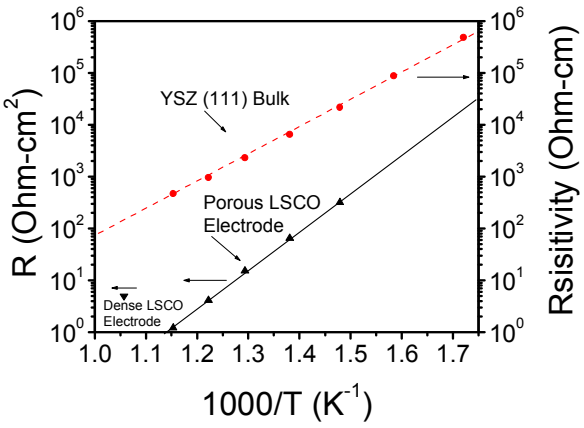

Fig.6 The YSZ resistivity and LSCO electrode area specific resistance obtained from the impedance measurement.

3 Conclusions

LSCO micro/nano composite thin films were successfully grown on a YSZ single crystalline substrate by pulsed laser deposition. Impedance spectroscopy showed low interface resistance, and lower area resistivity was observed for a porous/dense multi layer LSCO film than for a dense LSCO thin film. We have successfully used a porous electrode model to represent the micro-nano porous composite LSCO film with good experimental data fitting. This study suggests that the PLD-made multilayer LSCO film has a good potential for use as a cathode for intermediate temperature thin film solid oxide fuel cell applications. Further study is ongoing to optimize the structure of the micro-nano porous LSCO electrodes.

Acknowledgement

The authors thank Dr. A. J. Jacobson and L. Chen for their assistance. This work was partially supported by the Center for Advanced Materials, NASA, and the R. A. Welch Foundation.

References:

[1] J. Fleig, Solid Oxide Fuel Cell Cathodes, *Annual Review of Materials Research*, Vol.33, 2003, pp.361-382.

[2] X. Chen, N. J. Wu, L. Smith and A. Ignatiev, Thin-Film Heterostructure Solid Oxide Fuel Cells, *Applied Physics letters*, 2004, Vol.84, pp.2700-2702.

[3] X. Chen, N. J. Wu, D.L. Ritums and A. Ignatiev, Pulsed Laser Deposition of Conducting Porous La-Sr-Co-O Films, *Thin Solid Films*, Vol.342, 1999, pp.61-66.

[4] S. B. Adler, Mechanism and Kinetics of Oxygen Reduction on Porous $La_{1-X}Sr_xCoO_{3-\delta}$ Electrodes, *Solid State Ionics*, Vol.111, 1998, pp.125-134.

[5] X. Chen, N. J. Wu, L. Smith, J. R. Li, and A. Ignatiev, Ultra Thin Solid Oxide Fuel Cells with High Power Density, *WSEAS Transactions on Electronics*, Vol.3, 2006, pp.28-33.

[6] X. Chen, N. J. Wu, L. Smith, J. R. Li, A. Ignatiev, Thin Film Solid Oxide Fuel Cell for Lower Temperature Operations, 2005 WSEAS/IASME International Conference on ELECTROSCIENCE and TECHNOLOGY for NAVAL ENGINEERING and ALL-ELECTRIC SHIP (NAVAL' 05), Miami, Florida, USA, November 17-19, 2005.